

# Beyond Crash: Hijacking Your Autonomous Vehicle for Fun and Profit

Qi Sun Ahmed Abdo Luis Burbano<sup>†</sup> Ziyang Li

Yaxing Yao Alvaro Cardenas<sup>†</sup> Yinzhi Cao

*qsun28@jh.edu Ahmed.Abdo@jhuapl.edu ziyang@cs.jhu.edu,  
 {lburbano, alacarde}@ucsc.edu {yaxing, yinzhi.cao}@jhu.edu*  
*Johns Hopkins University <sup>†</sup>University of California, Santa Cruz*

## Abstract

Autonomous Vehicles (AVs), especially vision-based AVs, are rapidly being deployed without human operators. As AVs operate in safety-critical environments, understanding their robustness in an adversarial environment is an important research problem. Prior physical adversarial attacks on vision-based autonomous vehicles predominantly target immediate safety failures (e.g., a crash, a traffic-rule violation, or a transient lane departure) by inducing a short-lived perception or control error. This paper shows a qualitatively different risk: a long-horizon route integrity compromise, where an attacker gradually steers a victim AV away from its intended route and into an attacker-chosen destination while the victim continues to drive “normally.” This will not pose a danger to the victim vehicle itself, but also to potential passengers sitting inside the vehicle, who may not notice the route changes.

In this paper, we design and implement the first adversarial framework, called JACKZEBRA, that performs route-level hijacking of a vision-based end-to-end driving stack using a physically plausible attacker vehicle with a reconfigurable display mounted on the rear. The central challenge is temporal persistence: adversarial influence must remain effective in changing viewpoints, lighting, weather, traffic, and the victim’s continual replanning—without triggering conspicuous failures. Our key insight is to treat route hijacking as a closed-loop control problem and to convert adversarial patches into steering primitives that can be selected online via an interactive adjustment loop based on observed victim behavior. Our adversarial patches are also carefully designed against worst-case background and sensor variations so that the adversarial impacts on the victim, e.g., the changes of turning degrees, can be expected or estimated. Our evaluation shows that JACKZEBRA can successfully hijack victim vehicles to deviate from original routes and stop at places designated by the adversary with a high success rate.

## 1 Introduction

Autonomous Vehicles (AVs) [5] are self-driving systems designed to operate without continuous human control. Today, AV deployments have gone beyond prototypes to commercial operation on public roads: Waymo One runs a large-scale robotaxi service and is expanding to additional U.S. cities [32], while major robotaxi programs also operate outside the U.S., including Baidu’s Apollo Go [8]. In freight transportation, commercial driverless trucking has begun in limited corridors, exemplified by Aurora’s driverless customer deliveries in Texas [6]. A central enabling technology for many modern AV stacks is vision-based control, where camera observations are mapped to driving decisions by learned models (increasingly including vision-language-action architectures). Despite strong empirical performance, vision-based control remains vulnerable to adversarial manipulation, including physically realizable attacks, such as adversarial patches.

A substantial body of work has demonstrated attacks against vision-based AV pipelines. For instance, carefully crafted physical perturbations can cause a stop sign to be misread as a yield sign [12], and adversarial patches for traffic-sign recognition can be optimized to remain effective across viewing angles and distances [14]. Other studies show that adverse visual conditions can trigger unsafe behavior: dark scenes can induce deviation of routes and guardrail collisions [23], while dirty road patterns can mislead lane-centering and lane-change systems, potentially resulting in crashes [26]. Beyond static artifacts, adversarial vehicles that perform intentionally designed maneuvers can also induce dangerous outcomes such as pedestrian collisions or impacts [31]. However, despite their diversity, existing attacks share a common objective: to induce immediate short-term failures, such as crashes or overt violations of traffic-rules, rather than sustained long-term manipulation of the vehicle’s end-to-end route.

The central research question in this paper is whether the route of a vision-based AV can be *hijacked* by an adversary-controlled lead vehicle that displays a dynamically reconfig-

urable visual patch on its rear. In such an attack, the victim does not merely exhibit a transient error; instead, it is gradually redirected over a long horizon and ultimately driven toward an adversary-designated destination rather than its intended endpoint. This threat has clear safety implications in realistic settings—for example, when a passenger is unfamiliar with the city, does not actively monitor the route, or is otherwise unable to quickly recognize subtle deviations. In this case, route manipulation compromises not only vehicle autonomy but also passenger security by allowing unwanted relocation to a potentially unsafe area. From a research perspective, long-horizon route hijacking is also technically challenging. Unlike previous patch attacks that aim for immediate failures (e.g., a crash or a conspicuous violation of traffic-rules), route hijacking requires *precise, sustained and fine-grained* influence over the victim’s perception and control in many perception planning–actuation cycles, despite changes in perspective, distance, lighting, traffic and the victim’s continual replanning. Moreover, the attack must remain *stealthy*: the induced behavior should appear nominal to external observers and should avoid obvious anomalies or major rule violations (e.g., running red lights) that would reveal manipulation.

In this paper, we design and implement the first long-term hijacking framework, called JACKZEBRA, which adversarially controls a victim vision-based AV so that it safely drives to an adversary-controlled location, deviating from its originally-planned path and destination. Our key insight is an interactive adjustment loop, i.e., our adversarial vehicle monitors the differences of the victim’s behavior from our prediction using a back camera and then changes the adversarial patch accordingly to compensate for the differences. Intuitively, if JACKZEBRA wants to hijack the AV to turn left, but the AV does not turn left enough to follow the driving rule, JACKZEBRA will display a different patch with more turning angles to correct the victim’s behavior.

More specifically, the workflow of JACKZEBRA is as follows. First, at the offline planning stage, JACKZEBRA generates a database of adversarial patches, called a patch bank, with different capabilities (e.g., turning angles and directions) based on the map of a target town and its street views. Our adversarial patch generation adopts an offline min-max optimization against worst-case contextual perturbations in background scenes and sensor modalities so that the patches are robust under different lighting conditions, such as daytime and night, or weather, such as fogs and rains.

Then, at the online attack stage, JACKZEBRA plans an adversarial route, drives an adversary vehicle in front of the victim, and displays a pre-trained adversarial patch based on the map and the planned route. JACKZEBRA works on three tasks at the same time. First, JACKZEBRA keeps monitoring the behavior of the victim using a rear-facing camera and changes the adversarial patch in runtime using an algorithm taking the victim’s behavior as inputs to finish the interactive adjustment loop. Second, JACKZEBRA monitors the adversar-

ial vehicle itself using the GPS sensor so that it will be used to calculate the victim’s status and adjust the adversarial vehicle as well. Lastly, JACKZEBRA uses a front-facing camera to monitor the condition of the road and maneuver the adversarial vehicle according to traffic rules, e.g., traffic lights and stop signs, so that both adversarial and victim vehicles obey the rules.

The evaluation of JACKZEBRA is based on a simulation platform integrating the SimLingo driving agent [25], the Bench2Drive benchmark [16], and the CARLA simulator [2]. We evaluated JACKZEBRA against 39 original-adversarial route pairs, and the results show that JACKZEBRA successfully hijacked 34 out of 39 routes to mislead the victim vehicle to the adversary-designated location. Furthermore, JACKZEBRA successfully finishes 122.2 meters of route length on average. Our hijacking attack is stealthy: It is generally difficult to differentiate between benign AV driving and JACKZEBRA hijacking based on the trajectories, unsafe driving behaviors, and traffic rule violations.

**Contributions.** To summarize it, we make the following contributions in coming up with the attack and designing the JACKZEBRA framework:

- We propose the first, long-term, route-level, vision-based hijacking attack, which adversarially controls a victim vehicle to an adversary-designed place using another adversarial vehicle driving in the front.
- We design a min-max optimization training procedure against worst-case context and sensor variations to generate robust adversarial patches.
- We design patches as a persistent actuation primitive and implement a novel attack framework using an interactive adjustment loop, which monitors the victim’s behaviors and dynamically changes adversarial patches displayed on the back of the adversarial vehicle. Both our adversarial and the victim vehicles will follow traffic rules, e.g., stopping at a red light or a stop sign.
- Our evaluation shows that JACKZEBRA successfully hijacked 34 out of 39 routes with up to three different intersections deviating from the originally planned route of the victim vehicle.

## 2 Overview

We first describe vision-based AVs in Section 2.1, then use an example to describe the motivation of our attack in Section 2.2. Next, we present our threat model in Section 2.3 and lastly the overall system architecture of JACKZEBRA in Section 2.4.

### 2.1 Background

In this subsection, we provide background on vision-based autonomous vehicles. Figure 1 summarizes the overall pipeline; below, we describe its inputs, model architecture, and outputs.

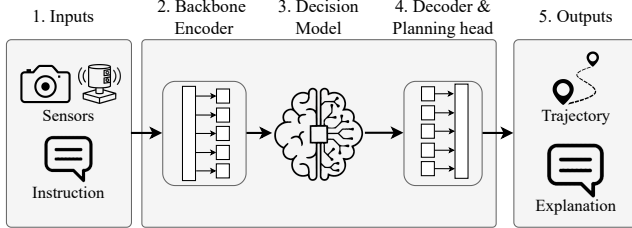


Figure 1: An overall workflow of an autonomous driving agent: Sensor observations (e.g., images), navigational commands, and language prompts are first provided as inputs (Step 1). A backbone encoder (Step 2) converts these multi-modal signals into a compact embedding representation (e.g., visual features and instruction tokens). The resulting embeddings are then consumed by a decision-making model (e.g., AV-based Vision Language Action model) that fuses perception with intent and contextual information to infer driving-relevant internal representations (Step 3). Its outputs are passed to a decoder and planning head (Step 4), which maps the fused representation into actionable predictions. Finally, the system produces two outputs (Step 5): a planned trajectory for vehicle control and a natural-language explanation that summarizes the rationale underlying the driving decision.

**Expected inputs.** As illustrated in Figure 1, a vision-based driving system, e.g., a vision-language-action driving system, consumes three main input streams: (i) sensor observations (e.g., front-facing camera images), (ii) navigational context (e.g., GPS target points or a high-level language command), and (iii) ego-state signals (e.g., vehicle speed and pose). These inputs provide complementary information about the environment, the intended route, and the current state of vehicle movement.

**Decision model.** A backbone encoder transforms the heterogeneous modalities into a shared embedding space (e.g., visual features and instruction tokens). The resulting embeddings are fused by a decision-making model that jointly conditions perception and task context, typically via a unified prompt-like sequence created by interleaving visual, navigation, and state embeddings into a common template. The fused representation is then processed by a decoder and planning head to generate driving-relevant predictions.

**Outputs.** The decision-making model produces (i) control-relevant action outputs and, optionally, (ii) natural-language explanations. For action prediction, many driving agent systems output future motion plans as waypoints instead of low-level steering and throttle. A common design predicts both temporal waypoints (indexed at fixed time intervals) and geometric path waypoints (indexed at fixed spatial intervals): temporal waypoints support speed planning, while geometric

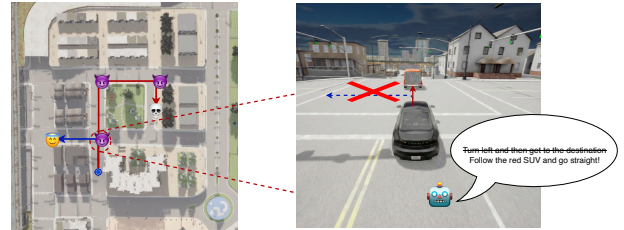


Figure 2: An illustration of JACKZEBRA’s motivation: A victim car is supposed to follow the blue route to a safe location, but is hijacked by an SUV to a different location. The left part shows the benign route (blue) and the adversarial route (red). The right part shows the scenario in a particular intersection: The victim is supposed to turn left, but was hijacked and instructed to go straight and follow the adversarial SUV.

waypoints stabilize lateral control during turning and obstacle avoidance. These trajectories are converted into steering and acceleration using standard feedback or closed-loop dynamics controllers (e.g., a proportional–integral–derivative (PID) controller) that track the predicted waypoint-derived targets. To satisfy real-time constraints, waypoint decoding is often implemented non-autoregressively (e.g., with learnable action queries and lightweight MLP heads) to predict waypoint offsets in a single forward pass.

## 2.2 Motivation

An end-to-end route-hijacking attack poses a significant real-world threat in autonomous ride-hailing settings. For example, a passenger may request an autonomous taxi to drive to a pre-determined destination in an unfamiliar city and have limited ability to detect subtle deviations in routing decisions. An adversary (e.g., operating a nearby vehicle) could manipulate the victim AV’s perception or decision pipeline so that it gradually departs from the intended route and ultimately navigates to an attacker-chosen location. Such an unauthorized redirection not only violates service integrity, but also introduces serious personal safety and security risks to the passenger, especially when the diversion occurs without obvious alarms or abrupt driving behaviors that would prompt immediate intervention.

In Figure 2, the victim AV begins the route that follows under its standard autonomy trajectory (the blue line), i.e., turning left at the first intersection. An attacker-controlled SUV then remains close and introduces JACKZEBRA, which is consistently seen by the front camera sensors of the victim AV over time. As the victim AV repeatedly replans in closed loop, these small incremental biases accumulate into a macroscopic route deviation: the vehicle continues to drive smoothly towards the planned trajectory (the red line), and executed path drifts away from the intended destination (the blue line) and converges towards an attacker chosen endpoint,

i.e., goes straight and then follows the red route to a different location. The figure thus emphasizes that the attack is not merely a momentary perception error, but a sustained closed-loop manipulation that translates into end-to-end navigation failure.

Although the high-level attack scenario appears intuitively simple, executing an end-to-end attack is challenging in practice because it requires temporal persistence, i.e., the adversarial influence must remain effective continuously over time and across many consecutive perception–decision–control cycles. Rather than causing a single-frame misclassification, the attacker must maintain a coherent bias under changing viewpoints, vehicle motion, lighting, and scene dynamics, while the AV repeatedly updates its plan and applies feedback corrections. A single failure can loosen the victim vehicle, leading to a crash or a return to the original route. Specifically, we summarize two major requirements for such temporal persistence.

- *Robustness across diverse environments*: The environments along the adversarial routes may encounter different road conditions, surrounding vehicles, traffic signals, pedestrian activity, light conditions, and weather changes (like rain and fog). The adversary needs to keep control of the victim across those different factors along the adversarial route.
- *Stealthiness*: While the victim’s car is under control of the adversary, it still needs to follow traffic rules and ensure the driving smoothness and passenger comfortableness. The purpose is to make the attack stealth so that it is hard to notice by either inside passengers or outside observers.

### 2.3 Threat Model

Our threat model assumes two parties as described below:

- *The victim Autonomous Vehicle*: The victim AV is equipped with a vision-based autonomous driving system in which a front-facing camera captures road scenes and provides the primary input for driving decisions. The vehicle may also incorporate auxiliary sensors (e.g. GPS) to support navigation and contextual reasoning, but the core decision-making pipeline is dominated by camera perception. We also assume an informed adversary who can infer the key properties of the deployed driving agent from the victim vehicle’s make, model and publicly available information, resulting in practical knowledge of the architecture and operating assumptions of the system.
- *The Adversary Autonomous Vehicle*: The adversary AV is another vehicle that drives in front of the victim AV and carries a reconfigurable rear-mounted display (e.g. a large screen) capable of rendering adversarial JACKZEBRA patches. The attacker AV is also equipped with on-board sensing (e.g. a rear-facing camera and LiDAR) to observe the relative position and driving behavior of the victim AV and to support closed-loop adjustment of the

displayed JACKZEBRA patches. This threat model is practically plausible because rear-mounted digital signage is increasingly common in advertising and fleet settings, allowing an attacker vehicle to appear as a normal car displaying dynamic advertisements while covertly deploying the adversarial JACKZEBRA attack.

**Out-of-scope Attacks.** We consider the following attack classes outside our scope:

- *Infrastructure manipulation*: attacks that modify or tamper with transportation infrastructure (e.g., traffic signs, lane markings, or traffic signals).
- *Physical-access attacks*: attacks requiring direct physical access to the vehicle (e.g., interfacing with the CAN bus via a wired plug-in device).
- *Sensor attacks*: attacks that directly target sensors (e.g., LiDAR, radar, or GPS spoofing/jamming).
- *Software exploitation*: attacks that rely on exploiting software/firmware vulnerabilities or other implementation defects.

### 2.4 System Architecture

Figure 3 represents the overall architecture of JACKZEBRA, which contains two major stages. The first stage (the left part of the figure) is performed offline to prepare a patch bank that contains a series of patches with different impacts on a victim car at different locations on a pre-set map, such as a target town or city. Specifically, JACKZEBRA takes Lidar, GPS, and street maps as input, perturbs all of them, and optimizes a group of patches for specific target behaviors such as turning left, turning right, and going straight.

The second stage (the right part of the figure), which is performed online, is to dynamically choose the patch from the patch bank on the back of an adversarial car based on the sensor inputs. Specifically, there are three types of sensors. First, the rear camera is used to monitor the behavior of the victim vehicle and calculate its status, e.g., whether it successfully follows instructions. Second, the front camera is used to help maneuver the adversarial vehicle so that it will follow traffic rules, e.g., stop signs and traffic lights. Lastly, the adversary calculates the deviation of itself from the adversarial routes based on its GPS sensor data. All three pieces of information are used together to choose the correct patch from the patch bank for the online hijacking attack.

JACKZEBRA achieves the temporal persistence required for end-to-end route hijacking by satisfying two different requirements. First, it constructs a patch bank via a Min–Max optimization procedure that explicitly adversariallyizes contextual variations: the optimizer searches over challenging background perturbations (e.g., weather, illumination, and viewpoint changes) while updating the patch to consistently induce the target decision. This formulation encourages patches to remain effective under diverse environmental conditions. Second, during deployment, JACKZEBRA employs an interactive

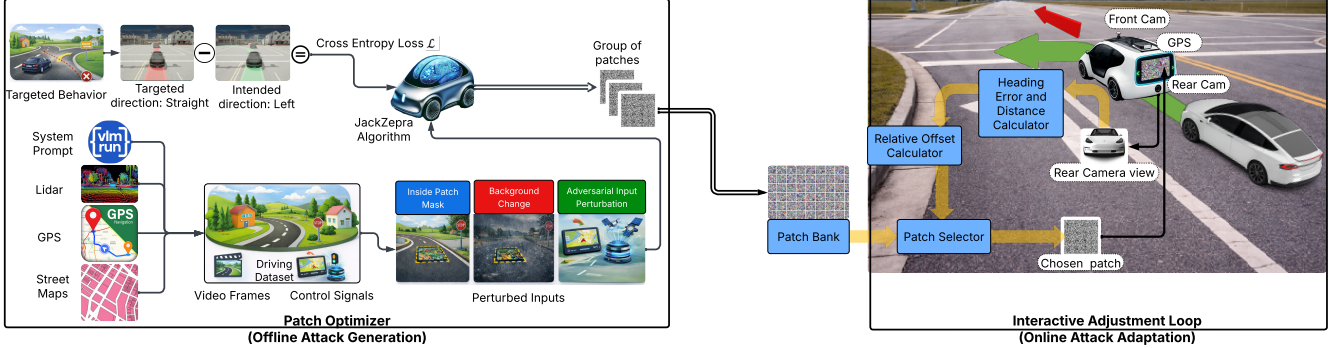


Figure 3: System Architecture. Note that JACKZEBRA has two major stages: (i) an offline attack generation stage to optimize a bank with patches with different hijacking purposes, e.g., turning angles, and (ii) an online attack stage to adjust the victim car using a chosen image based on three types of sensors, including front- and back-facing cameras and GPS locations. Both the adversarial and the victim vehicles are under the influence of JACKZEBRA: the adversarial vehicle is instructed by JACKZEBRA to follow traffic rules, and the victim vehicle is influenced by the chosen patch on the adversarial vehicle.

adjustment loop that updates the patch displayed online using feedback derived from the onboard sensors of the attacker vehicle and the observed behavior of the victim AV. By adapting the patch in response to runtime conditions, the attack maintains its influence over time while maintaining stealthy, traffic-compliant driving behavior.

### 3 Design

This section presents the design of JACKZEBRA, which comprises two stages. We first describe Stage 1, the offline patch optimization procedure in Section 3.1. We then detail Stage 2, the interactive online adjustment loop used during the execution of the attack, in Section 3.2.

#### 3.1 Offline Attack Stage (1): Patch Optimization

Stage 1 of JACKZEBRA constructs a patch bank  $\mathbf{P}$  using driving scenes collected on a target map. The key objective is to learn patches that remain effective under realistic environmental variability by adopting a Min–Max optimization framework that explicitly adversarializes context during training. Intuitively, JACKZEBRA changes the context, i.e., the background and control signals, against the patch, so that it remains effective in the worst-case contextual perturbations. This stage consists of two main components: (i) generating context perturbations and (ii) solving the resulting Min–Max optimization problem, as described next.

**Context perturbation.** Consider a benign driving sample  $(\mathbf{V}_d, \mathbf{S}_d)$ , where  $\mathbf{V}_d \in \mathbb{R}^{H \times W \times C}$  denotes visual input (e.g., an RGB frame or a sequence of camera frames) with height  $H$ , width  $W$  and  $C$  channels. The term  $\mathbf{S}_d$  denotes the accompanying auxiliary and control signals consumed by the

victim model, such as GPS-derived target points, navigation commands, traffic-light or route context, LiDAR-derived features or other non-RGB channels. Then, given a binary mask  $m \in \{0, 1\}^{H \times W}$  and a patch  $\delta \in \mathbb{R}^{H \times W \times C}$ , the patched visual input is in Equation 1:

$$\tilde{\mathbf{V}} = \mathbf{V}_d \odot (1 - m) + \delta \odot m, \quad (1)$$

where  $\odot$  denotes elementwise multiplication. We then describe two additional learnable perturbations:

- $\delta_b$  for the *background* region  $\mathbf{V}_d \odot (1 - m)$ ,
- $\delta_s$  for the *control signals*  $\mathbf{S}_d$  (e.g., GPS, LiDAR, or navigation commands). Accordingly, the perturbated control signal  $\tilde{\mathbf{S}} = \mathbf{S}_d + \delta_s$

The perturbed input becomes Equation 2:

$$(\tilde{\mathbf{V}}, \tilde{\mathbf{S}}) = ((\mathbf{V}_d + \delta_b) \odot (1 - m) + \delta \odot m, \mathbf{S}_d + \delta_s), \quad (2)$$

where  $\delta_b$  and  $\delta_s$  are projected into bounded  $\ell_\infty$  balls to preserve realism.

**Min–Max formulation.** Let  $\mathbf{y} = (y_1, \dots, y_T)$  denote the output sequence of the model (e.g., predicted waypoints coordinates), and  $\mathbf{y} = f(\tilde{\mathbf{V}}, \tilde{\mathbf{S}})$  after context perturbation. Let  $\mathbf{y}^* = (y_1^*, \dots, y_T^*)$  denote the target output sequence. Let  $\mathcal{L}(\mathbf{y}^*, \mathbf{y})$  denote the cross-entropy between the target and the victim model's predictions:

$$\mathcal{L}(\mathbf{y}^*, \mathbf{y}) = \mathcal{L}(\mathbf{y}^*, f(\tilde{\mathbf{V}}, \tilde{\mathbf{S}})) = - \sum_{t=1}^T \log p_f(y_t^* | y_{<t}^*, \tilde{\mathbf{V}}, \tilde{\mathbf{S}}) \quad (3)$$

A standard targeted patch attack solves the object in Equation 4:

$$\min_{\delta} \mathbb{E}_{(\mathbf{V}_d, \mathbf{S}_d)} \mathcal{L}(\mathbf{y}^*, f(\tilde{\mathbf{V}}, \tilde{\mathbf{S}})) \quad (4)$$

That is,  $(\delta_b, \delta_s)$  is an *adversarial context player* that tries to find the hardest background and signal configuration for the

current patch. This leads to the following min-max objective in Equation 5:

$$\min_{\delta} \max_{\delta_b, \delta_s} \mathcal{L}(\mathbf{y}^*, f((\mathbf{V}_d + \delta_b) \odot (1 - m) + \delta \odot m, \mathbf{S}_d + \delta_s)), \quad (5)$$

The Algorithm 1 summarizes the procedure in Stage 1 of JACKZEBRA. Line 1 specifies the inputs: a driving data set  $D$ , a target behavior  $\mathbf{y}^*$  (e.g., a targeted incorrect intent such as *turn-right*) and a binary mask  $m$  that defines the patch placement in the image (with  $m=1$  in the patch region and  $m=0$  elsewhere). Line 2 defines the variables optimized during training: the adversarial patch  $\delta$ , which modifies only pixels within the masked region; a background perturbation  $\delta_b$ , applied exclusively to the non-patch area to emulate variations in the surrounding scene; and a signal perturbation  $\delta_s$ , applied to the auxiliary inputs  $\mathbf{S}_d$  to capture noise or distribution shift in non-visual channels. Finally, Line 3 lists the optimization hyperparameters, including the learning rates  $\alpha$ ,  $\alpha_b$ , and  $\alpha_s$  for  $\delta$ ,  $\delta_b$ , and  $\delta_s$ , respectively, and the context-maximization interval  $N$ , which controls the update frequency:  $\delta$  is updated for  $N$  steps per iteration, while  $\delta_b$  and  $\delta_s$  are updated once to adversarially refresh the context.

We next detail the optimization procedure. At each iteration, JACKZEBRA samples a driving instance  $(\mathbf{V}_d, \mathbf{S}_d)$  from the data set  $D$  (Line 5), thus exposing the training to heterogeneous conditions (e.g., routes, weather and traffic) between iterations. This sampling strategy is analogous to an Expectation-over-Transformation (EoT) objective, in that it implicitly optimizes the patch over a distribution of temporal and environmental variations. Given the sample instance, JACKZEBRA constructs the perturbed inputs by applying the visual and auxiliary perturbations to  $(\mathbf{V}_d, \mathbf{S}_d)$  (Lines 6–7), and then evaluates the corresponding attack loss (Line 8). Then, JACKZEBRA alternates between:

- Inner Optimization (Lines 9–12): Context maximization. For fixed  $\delta$ , JACKZEBRA performs *gradient ascent* on  $\delta_b$  (Line 10) and  $\delta_s$  (Line 11) to maximize the loss, yielding a worst-case context for the current patch.
- Outer Optimization (Lines 13): PGD-based patch minimization. For the resulting worst-case context, JACKZEBRA takes a *gradient descent* step on  $\delta$  to reduce the loss at Line 13, making the patch more robust to difficult contexts.

Finally, in Line 15, JACKZEBRA returns the optimized patch  $\delta$ , trained to remain effective across many sampled scenes and under adversarially chosen worst-case variations of both background appearance and auxiliary/control inputs. Note that this is an optimization of a single patch  $\delta$  for one target direction  $\mathbf{y}^*$  (e.g., waypoints to turn left 5 degrees). To enable continuous steering control during the attack, JACKZEBRA constructs a patch bank  $\mathcal{P} = \{\delta^{(1)}, \delta^{(2)}, \dots, \delta^{(M)}\}$  repeating the optimization for  $M$  discrete steering directions, each with a corresponding target output  $\mathbf{y}^{*(i)}$ .

---

#### Algorithm 1 Offline Patch Min-max Optimization

---

```

1: Input: driving dataset  $D = \{(\mathbf{V}_d, \mathbf{S}_d)\}$ , target  $\mathbf{y}^*$ , mask
    $m$ 
2: Initialize patch  $\delta$ , background perturbation  $\delta_b$ , signal perturbation  $\delta_s$ 
3: Hyperparameters Learning rate  $\alpha$ ,  $\alpha_b$ , and  $\alpha_s$  for  $\delta$ ,  $\delta_b$ ,  $\delta_s$  respectively, context maximization interval  $N$ .
4: for  $k = 1$  to  $K$  do
5:   Sample  $(\mathbf{V}_d, \mathbf{S}_d)$  from  $D$ 
6:    $\tilde{\mathbf{V}} \leftarrow (\mathbf{V}_d + \delta_b) \odot (1 - m) + \delta \odot m$ 
7:    $\tilde{\mathbf{S}} \leftarrow \mathbf{S}_d + \delta_s$ 
8:    $\mathcal{L} \leftarrow -\sum_{t=1}^T \log p_f(y_t^* | y_{<t}^*, \tilde{\mathbf{V}}, \tilde{\mathbf{S}})$ 
9:   if  $\text{mod}(k, N) == 0$  then  $\triangleright$  Context Maximization
10:     $\delta_b \leftarrow \delta_b + \alpha_b \nabla_{\delta_b} \mathcal{L}$ 
11:     $\delta_s \leftarrow \delta_s + \alpha_s \nabla_{\delta_s} \mathcal{L}$ 
12:   end if
13:    $\delta \leftarrow \delta - \alpha \nabla_{\delta} \mathcal{L}$   $\triangleright$  Patch minimization
14: end for
15: return optimized patch  $\delta$ 

```

---

### 3.2 Online Attack Stage (2): Interactive Adjustment Loop

Stage 2 of JACKZEBRA adapts the patch displayed on the adversary vehicle through an interactive adjustment loop that leverages real-time deviations of both the adversary and victim vehicles with respect to the attacker-chosen route. As illustrated in Fig. 4, JACKZEBRA continuously collects measurements from the adversary vehicle’s GPS and rear-facing camera and derives a set of geometric quantities. The key idea is to estimate the relative state of each vehicle with respect to the adversarial path, including the lateral distance to the path and the alignment of the direction (i.e., the relative angle of yaw/heading). Tracking both vehicles is necessary because the adversary can intentionally deviate from the nominal route (e.g. to remain in view and preserve influence over the victim), and such a motion affects the relative geometry of the victim and consequently the required patch selection. Using these estimates of relative distance/heading, JACKZEBRA selects (and updates) the most appropriate patch to sustain the intended hijacking effect while maintaining stealth. Next, we detail how JACKZEBRA computes (i) the deviation status of the adversary vehicle and (ii) the relative status of the victim vehicle from these sensor observations.

**Adversarial Vehicle Deviation Status:** JACKZEBRA calculates the position of the adversarial vehicle relative to the pre-planned adversarial route. Let us assume that the adversarial route is represented as an ordered sequence of coordination  $\mathbf{W} = w_1, w_2, \dots, w_n$ , where  $w_i = (x_i, y_i)$ . Given the attacker’s current position  $\vec{p} = (x_p, y_p)$ , JACKZEBRA finds the nearest waypoint  $w_i$  and its next waypoint  $w_{i+1}$ , and projects  $\vec{p}$  on the line between  $w_i$  and  $w_{i+1}$  to find  $\vec{q} = (x_q, y_q)$ . Then, JACKZEBRA

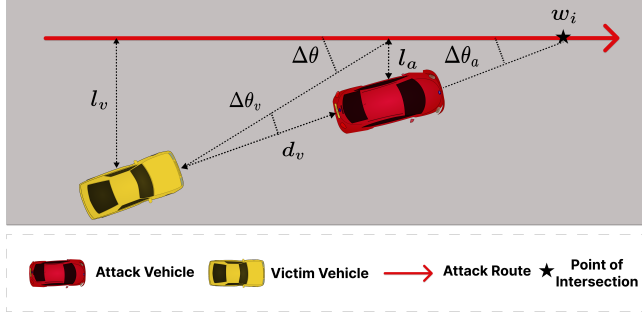


Figure 4: An illustration of Adversarial and Victim Vehicle and Their Positions Related to the Adversarial Route. JACKZEBRA uses such information to choose a patch to display on the back of the adversarial vehicle (i.e., the red vehicle).

BRA represents the adversarial vehicle deviation status using two variables:

- Adversarial Vehicle’s lateral offset  $l_a$ . The lateral distance from the attacker’s position to the route is denoted in Equation 6 below:

$$l_a = |\vec{p} - \vec{q}| \quad (6)$$

- Adversarial Vehicle’s heading error  $\Delta\theta_a$ . We have the angular difference between the attacker’s heading  $\theta_a$  and the route direction in Equation 7:

$$\Delta\theta_a = \theta_a - \text{atan2}(y_{i+1} - y_i, x_{i+1} - x_i) \quad (7)$$

**Victim Vehicle Relative Status:** JACKZEBRA monitors the relative position of the victim vehicle using a rear-facing camera mounted on the adversarial vehicle. Specifically, a real-time object detector identifies the victim vehicle in the camera frame with a bounding box  $\mathbf{B} = (u, v, w, h)$ , where  $u, v$  is the coordination of the center of the box and  $(w, h)$  are the width and height in pixels. Then, JACKZEBRA calculates the victim vehicle’s status using the following variables:

- Relative distance  $d_v$  between the victim and the adversarial vehicles. JACKZEBRA estimates the distance  $d_v$  to the victim from the bounding box size, assuming a known reference vehicle width  $w_v$  and  $f$  the focal length of the camera in pixels, we have a definition of  $d_v$  in Equation 8:

$$d_v = \frac{f \cdot w_v}{w} \quad (8)$$

- Heading error ( $\Delta\theta_v$ ) of the victim relative to the adversary’s centerline. Assuming the victim’s heading error as  $\Delta\theta_v$  and the center of the entire rear image as  $u_c$ , we have Equation 9:

$$\Delta\theta_v = \arctan\left(\frac{u - u_c}{f}\right) \quad (9)$$

**Patch Selection:** At each time step, JACKZEBRA selects a patch from the patch bank  $\mathbf{P}$  based on where the victim is currently relative to the adversarial route. This requires two inputs: the victim’s lateral offset  $l_v$  from the adversarial route (Equation 10) and its heading error  $\Delta\theta_v$  relative to the direction of the route (Equation 11):

$$l_v = l_a + d_v \cdot \sin(\Delta\theta_v) \quad (10)$$

$$\Delta\theta = \Delta\theta_a + \Delta\theta_v \quad (11)$$

where  $l_a$  and  $\Delta\theta_a$  are the offset and heading error of the adversarial vehicle (Equations 6–7), and  $d_v$  and  $\Delta\theta_v$  are the relative distance and heading error of the victim (Equations 8–9).

Given  $l_v$  and  $\Delta\theta$ , JACKZEBRA then computes a desired steering correction in Equation 12:

$$\Delta\phi = -k_l \cdot l_v - k_\theta \cdot \Delta\theta \quad (12)$$

where  $k_l$  and  $k_\theta$  are pre-set coefficients. Intuitively, this correction points the victim back toward the adversarial route. Lastly, JACKZEBRA selects a patch from  $\mathbf{P}$  that optimized the steering direction to match the most closely  $\Delta\phi$  for the display on the back of the adversarial vehicle.

**Adversarial Vehicle Maneuver:** JACKZEBRA also controls the adversary vehicle using a front-facing camera to monitor the road in real time. The objective is to preserve outwardly normal driving behavior for both the adversary and the victim, so that external observers and onboard passengers are unlikely to perceive anomalous behavior even while the victim is under attack. In particular, when JACKZEBRA detects regulatory cues such as a red traffic light or a stop sign, the adversary vehicle brakes to a compliant stop and temporarily disables the rear display (i.e., removes the adversarial patch), thus pausing the attack. In the absence of active influence, the victim vehicle reverts to its nominal driving policy and follows traffic control as usual. After the roadway becomes clear, the adversary vehicle resumes movement and re-establishes an effective following configuration by adjusting its distance and relative heading with respect to the victim, using the victim’s estimated position and orientation (Equations 10 and 9). Once the appropriate geometry is restored, the adversary vehicle re-enables the rear display and renders the patch selected by the patch-selection module to continue the attack.

## 4 Implementation

We implement an open-source version of JACKZEBRA in approximately 3,400 lines of Python. The implementation consists of two main components together with both vehicles. We describe our implementation details below.

**Patch Optimizer (The offline attack execution):** JACKZEBRA optimizes adversarial patches using the Adam optimizer with a learning rate of  $2/255$  from scratch and  $0.5/255$  for fine-tuning. Each patch is optimized for 1,000 iterations with fine-tuning from an existing patch. We use Adam for patch optimization because the objective is high-dimensional and highly non-convex, and gradients are often noisy due to stochastic sampling of driving frames and context variations (e.g., viewpoint and illumination). Adam’s adaptive learning rates per-parameter and momentum terms stabilize optimization under such heterogeneous gradient scales, allowing rapid progress from random initialization while reducing sensitivity to manual step-size tuning. The training data contains street views and GPS signals from benign routes. JACKZEBRA trains patches for five steering directions  $\{-18, -6, 0, 6, 18\}$  degrees, where zero means straight, negative values mean steering left, and positive values steering right, using six frames per direction sampled from collected driving data. Note that the patch optimizer is implemented in approximately 1,400 lines of Python using PyTorch 2.3, OpenCV 4.9, and Pillow 10.3.

**Interactive Adjustment Loop (The online attack execution):** The interactive adjustment loop runs as a lightweight feedback controller during the online attack. JACKZEBRA uses a proportional gain  $k_l = 0.3$  to compute the steering correction signal from the lateral offset of the victim and the head error and retrieves the nearest matching patch from the patch bank. To avoid frequent patch switching, caused by small fluctuations, JACKZEBRA uses a threshold of four degrees, i.e., the patch selector only switches to a new patch when the change in desired steering angle exceeds approximately 4 degrees. We implemented an interactive adjustment loop in approximately 600 lines of Python using NumPy 1.26.

**Adversarial and Victim Autonomous Vehicles:** The victim AV is controlled by an end-to-end autonomous driving agent equipped with a front-facing RGB camera ( $1920 \times 960$ ,  $110^\circ$  FOV), a GNSS receiver, an IMU, and a speedometer. The agent feeds camera frames and sensor data through a vision encoder and a multi-modal fuser. Then, the intermediate output will be fed to the decision model that jointly produces the steering, throttle, and brake commands at each time step.

The adversarial vehicle operates in an autopilot mode that keeps it approximately 12 m ahead of the victim along the victim’s forward direction. The auto-agent continuously adjusts the adversarial vehicle’s speed to match the victim’s velocity while maintaining the target following distance. The implementation of adversarial and victim vehicles is around 1500 lines of PyTorch 2.2, Transformers 4.46, and NumPy 1.23.

Table 1: Adversarial Route Statistics. The dataset contains three types of adversarial routes with intersections ranging from one to three. Each adversarial maps to a benign route, and all the driving decisions at the intersection are different. There are 13 benign routes in total and 39 adversarial routes.

# Intersections	# Routes	Avg. Length (m)
1	13	67.9
2	13	134.6
3	13	175.4

## 5 Evaluation

In this section, we first describe our experimental setup in Section 5.1 and then describe each research question from Section 5.2 to Section 5.4.

### 5.1 Experimental Setup

We describe in detail how our experiments are set up in the following.

**Hardware:** Our Stage 1 experiments are conducted on a cluster with NVIDIA A100 (80 GB) GPUs using PyTorch 2.3 with CUDA 12.5. Our Stage 2 experiments are on a single local 3090 workstation and comfortably maintains the 20–30 Hz camera rate.

**Victim Autonomous Vehicle:** The victim AV adopts SimLingo as the base autonomous driving agent [25], which combines an InternVL-style vision encoder with a LoRA-tuned LLM backbone and a disentangled waypoint decoder that outputs future trajectory waypoints for steering and speed regulation. All hyperparameters (e.g., visual encoder resolution, LLM temperature, waypoint horizon, tokenization scheme) remain at their default values. The underlying simulator is CARLA 0.9.15.

**Autonomous Driving Datasets and Benchmarks:** Our dataset is based on Bench2Drive [16], a suite of scenario-driven, closed-loop tasks designed to stress-test perception, reasoning, and planning modules under realistic driving conditions. We randomly sample 13 benign routes with town maps consisting of multiple intersections from the benchmark without modifications. Then, three adversarial routes are generated from the starting point of the benign routes. Specifically, at each intersection, we choose two directions that are different from the benign route and where the victim vehicle comes from. One adversarial route ends at the second intersection, and we will repeat the procedure for the other adversarial route to choose another two possible directions at the next intersection. In the end, the statistics of adversarial routes is shown in Table 1: Each benign route has three adversarial routes with intersections ranging from one to three. The turning direction at each intersection is different from the

benign route. We also list the average length of routes in each category in Table 1.

**Evaluation Metrics:** We use the following metrics in the experiment.

- **Hijacking Success Rate (HSR).** A successful hijack is defined as the victim reaching the adversary designated area with in a small radius ( $r$ ), e.g., 6 meters, before a timeout ( $T$ ), e.g., 10 minutes. Then, HSR is the percentage of successful hijacks among all trials.
- **Hijacking Compliance Length (HCL) and Hijacking Compliance Rate (HCR).** HCL is defined as the maximum length of the victim vehicle following the adversarial route, and HCR is the ratio of the HCL and the total adversarial route length.
- **Traffic Rule Violations.** This is defined as the number of violations against traffic rules, e.g., stop signs and red light. We use the number of violations as the metric, and divide it into either a red light or a stop sign violation.
- **Trajectory Curvature.** Curvature measures how sharply a vehicle’s trajectory, i.e., a geometric curve, is. It is defined as the rate of change of the tangent angle with respect to arc length.
- **Number of Hard Breaks.** A hard break is defined as a sudden, intense deceleration of a vehicle. Specifically, we define a hard break as a deceleration of more than  $3m/s^2$ , i.e., about  $6.7miles/h/s$ , following common definitions [1].
- **Number of Steer Reversals.** A steer reversal is a change in the direction of steering input, i.e., moving the steering wheel from one direction (e.g., left) to the opposite direction (e.g., right).

**Research Questions.** We answer the following research questions in the rest of evaluation.

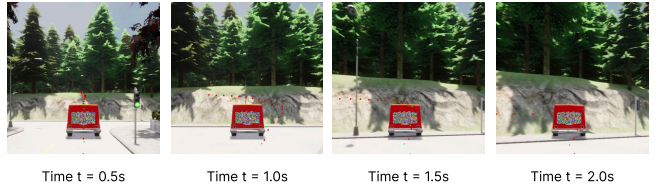
- **RQ1: Attack Reliability.** Can the attacker reliably hijack the victim to a malicious destination over long horizons? (Or in other words, what is the hijacking success rate of JACKZEBRA?)
- **RQ2: Attack Robustness.** How robust is the hijack under environmental shifts, e.g., weather and lighting conditions?
- **RQ3: Stealthiness.** Is the hijacking stealthy, i.e., whether the driving behaviors of the victim under hijacking are similar to those of a normal autonomous vehicle without being attacked?

## 5.2 RQ1: Overall Hijacking Reliability

In this research question, we evaluate the overall hijacking reliability in terms of HSR, HCL, and HCR against all adversarial routes in Table 1. Our overall results are shown in Table 2: JACKZEBRA successfully hijacked 34 out of 39 routes with an average hijacking complete rate of 91.4%. An



(a) Case Study 1: The victim vehicle is supposed to turn left at the intersection, but is redirected to go straight by JACKZEBRA.



(b) Case Study 2: JACKZEBRA fails to maneuver both adversarial and victim vehicles to make a sharp turn with 135 degrees.

Figure 5: An illustration of two case studies, one success (a) and one failure (b). The red and blue dots are victim vehicle’s predicted trajectories. The red dots are path waypoints depicting victim’s future position, and blue dots are speed waypoints depicting victim’s future speed.

immediate observation is that the hijacking success rate decreases as the number of intersections on the route increases. The reason is that hijacking difficulty becomes harder when the victim vehicle deviates more from the original path, because it always wants to go back to the original route based on its own calculation.

Note that there are five failure cases in total, and here are the reasons. First, there are two that are due to a software crash of the underlying CARLA framework. It might be a software bug in either CARLA or our code that needs to be fixed. Second, JACKZEBRA fails to adversarially manipulate the victim in three cases because the turn is larger than 90 degrees, e.g., sometimes 135 degrees. In those cases, the victim vehicle will not follow the adversarial route. We have a detailed example in our Case Study 2 to illustrate this failure.

### 5.2.1 Case Studies

We illustrate two case studies in this subsection.

**Case Study 1:** A vehicle successfully hijacked to the adversarial destination. Figure 5 (a) shows a representative successful hijack on an one-intersection route. The victim vehicle’s benign route requires a left turn at the upcoming intersection, while the adversarial route instructs the victim to continue straight. At  $t=0.5s$ , the adversarial vehicle merges in front of the victim and displays an initial patch for straight-line following. As both vehicles approach the intersection ( $t=1s$ ), the interactive adjustment loop detects a slight leftward drift in the victim’s heading, which is consistent with its internal navigation that planned to turn left. In response,

the interactive loop switches to a patch optimized for a right steering correction of approximately  $6^\circ$  to reduce the victim’s intent. At  $t=1.5s$ , the victim passes through the intersection going straight, and is fully committed to the adversarial route. The adversarial vehicle then reverts to the neutral ( $0^\circ$ ) patch to maintain lane centering. At  $t = 2s$ , the victim arrives within the 6-meter acceptance radius of the adversary-designated destination, and JackZebra completes the hijack. Throughout the process, the victim obeys all traffic signals (green light), maintains a comfortable speed profile, and does not make any sharp steering changes, which demonstrate that JackZebra is both effective and stealthy.

**Case Study 2:** A victim vehicle failing to make a big turn and then follow the adversarial route. Figure 5 (b) shows a failure case where the victim is hijacked to make a sharp right turn at the intersection, but fails to complete the maneuver. At  $t = 0.5s$ , the adversarial vehicle positions itself in front of the victim and displays a patch optimized for a right turning of  $20^\circ$ , which is the maximum angle in the patch bank. As both vehicles approach the intersection at  $t=1s$ , JACKZEBRA continuously selects the  $20^\circ$  patch to induce the sharpest right turn. However, at  $t=1.5s$ , the victim begins the turn but cannot complete it. Because the patch’s steering influence is insufficient to achieve such a sharp heading change within the narrow intersection range. At  $t=2s$ , both vehicles stop at the intersection, unable to proceed along the adversarial route.

The main reason for the failure is that the turning angle at this intersection of the adversarial route is 135 degrees to the right, which is larger than 90 degrees. Usually, such a big turn requires a left turn first and then a right turn. Currently, JACKZEBRA is not designed with such a mechanism to make left and right turns for the victim vehicle. Because the adversarial vehicle needs to maintain a relative position with the victim vehicle, the adversarial vehicle also fails to make such a big turn.

There are two possible solutions for this situation. First, when the adversary designs an adversarial route, they may avoid making such a big turn. Instead, the adversary may always try to find a detour that skips the intersection. In this specific case, the adversary can let the victim to turn left first, following the original route, and then hijack the vehicle at the next intersection to go around and reach the final destination. Second, as part of the future work, the adversary may first select patches with left then right turns, to achieve the final purpose of a big turn or even a U-turn.

**Takeaway for RQ1:** JACKZEBRA successfully hijacked victim vehicles to follow 34 out of 39 adversarial routes, a high hijacking success rate. The failure cases are due to sharp turns, e.g., those larger than 135 degrees, which can be avoided using detours to follow smooth turns.

Table 2: [RQ1] Hijacking reliability results. HSR means Hijacking Success Rate, HCR Hijacking Compliance Rate, and HCL Hijacking Compliance Length.

# Intersections	HSR $\uparrow$	HCR (%) $\uparrow$	HCL (m) $\uparrow$
1	12/13	$95.4 \pm 8.7$	$64.8 \pm 5.9$
2	12/13	$93.7 \pm 11.9$	$128.2 \pm 16.3$
3	10/13	$85.1 \pm 17.0$	$173.6 \pm 34.7$
Overall	34/39	$91.4 \pm 7.6$	$122.2 \pm 19.1$

### 5.3 RQ2: Environmental Shifts

In this research question, we evaluate how environmental shifts affect the hijacking completion rate on a randomly picked adversarial route. There are two main factors: (i) weather and lighting conditions, and (ii) traffic volume.

First, we follow the setting of existing works [31] to evaluate JACKZEBRA under 14 environmental conditions of different weather and lighting combinations. Our experiment leverages four different weather parameters: Sun altitude angle ( $S$ ), Cloudiness ( $C$ ), Precipitation on the ground ( $P_g$ ), and Precipitation in the air ( $P_a$ ). Figure 6 shows the HCR under different weather conditions: JACKZEBRA achieves 100% hijacking compliance rate except for three scenarios.

Figure 7 illustrates the three failure scenarios in detail. We identify two distinct failure modes:

- *Perception blur induced by hard rain.* Figures 7(a) and (b) show failures under hard rain conditions at noon and sunset, respectively. In both cases, heavy precipitation on the ground  $P_g$  and precipitation on the air  $P_a$  introduces significant visual compromise. The perception from victim’s front camera is blurred and distorted by the accumulated water, and the rain between the two vehicles produces motion blur that hides patch details. As a result, the victim’s camera cannot clearly capture the patch, compromising the adversarial impact of the patch.
- *Color shift induced by lighting.* Figures 7(c) shows the failure resulted under cloudy sunset condition. Unlike the hard raining scenarios, the victim has clear vision. However, the low sun altitude angle  $S$  creates a directional reflection towards the back of the adversarial vehicle. As shown in  $t = 0.5$  and  $t = 1$ , once the adversarial vehicle maneuvers through the intersection, its orientation relative to the sun changes, causing a specular reflection. From the perspective of the victim, this reflection causes a temporary color shift, especially for the adversarial patch. This dynamic color shift causes the victim’s vision encoder to perceive a different feature distribution, destroying the adversarial context that the patch was trained to induce.

Second, we evaluate JACKZEBRA’s robustness with different traffic volumes. Specifically, we test JACKZEBRA with three different volumes, i.e., (i) heavy: 4 vehicles per lane, 12 per junction, (ii) medium: 2 per lane, 6 per junction, and (iii)

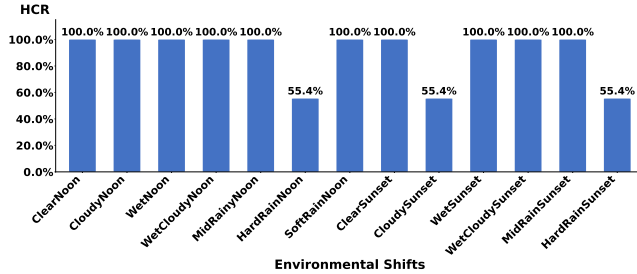


Figure 6: HCR across different environmental shifts.

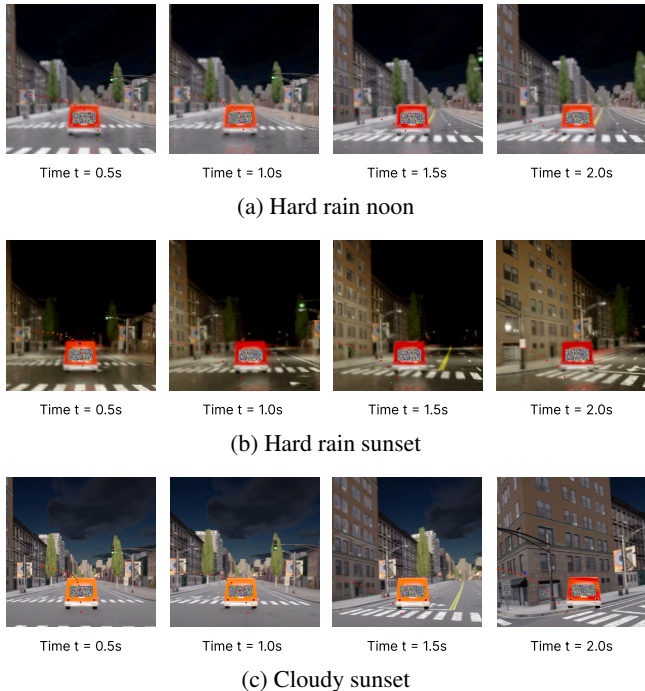


Figure 7: An illustration of failed hijacks under different environmental shifts.

light: 1 per lane, 2 per junction. Table 3 shows the HCR under these different traffic volumes: JACKZEBRA can successfully hijack a victim vehicle even if there is heavy traffic on the street. The reason is that the min-max algorithm used in the offline optimization stage has already considered different traffic volumes. That is, the chosen patch is effect regardless of the number of other vehicles on the road.

**Takeaway for RQ2:** JACKZEBRA is most robust under environmental shifts, e.g., changes in lighting conditions, weather, and traffic volumes. The failure cases are due to (i) perception blurs and (ii) color shifts, which are challenging cases for normal autonomous driving as well.

Table 3: HCR across different traffic volumes. Criteria columns show the number of vehicles per lane (#Veh./Lane), per junction (#Veh./Junction), and the spacing between vehicles. JACKZEBRA achieves 100% HCR for all scenarios.

Traffic	Criteria			HCR (%) ↑
	#Veh./Lane	#Veh./Junction	Spacing	
Light	2	2	25m	100
Medium	4	6	15m	100
Heavy	8	12	10m	100

#### 5.4 RQ3: Stealthiness

In this research question, we evaluate whether the hijacking attack is stealthy. Our high-level evaluation method is to compare adversarial hijacking, i.e., the behavior of the victim vehicle under the attack of JACKZEBRA, with benign driving, i.e., the behavior of the victim vehicle if it is planned to follow the adversarial route. The closer adversarial hijacking is to benign driving, the stealthier the hijacking attack is. The reason is that one may think that the victim vehicle is programmed to follow the adversarial route instead of being hijacked by JACKZEBRA. More specifically, we use two types of metrics: (i) trajectory smoothness and unsafe driving behaviors along the trajectory, and (ii) the number of safety rule violations.

Table 4 shows the average number and the value range of the trajectory curvature, number of hard brakes, and number of steer reversals. The high-level observation is that all metrics of adversarial hijacking are lower than those of benign driving, and the value range of adversarial hijacking is a superset of that of benign driving. Now, let us look at each factor individually. First, the curvature of adversarial hijacking is low because JACKZEBRA directs the victim to follow an adversarial route with a low curvature in general. Second, the number of hard brakes is small because there is another adversarial vehicle in front of the victim, which tries to maintain a constant distance. Therefore, there is no need for frequent hard brakes during driving. Lastly, the number of steer reversals is also small because of the nature of the designed adversarial routes and the hijacking algorithm of JACKZEBRA, which tries to avoid steer reversals as they are hard to manipulate.

Then, Table 5 shows the number of traffic rule violations in both benign driving and adversarial hijacking for the same route. The number of red light violations is zero for these two scenarios. As a comparison, adversarial hijacking has two violations of stop signs, while benign driving has zero. The reason is that obeying stop signs is generally harder than obeying traffic light. Here is the reason. When there is a red light, both the adversarial and the victim vehicles need to stop. Then, when the light turns green, both vehicles will start to go through the green light. On the contrary, when there is a stop sign, similarly both vehicles stop. Then, when the adversarial

Table 4: A comparison of trajectory smoothness and unsafe driving behaviors between benign driving and adversarial hijacking under the influence of JACKZEBRA.

Metric	Benign Driving		Adversarial Hijacking	
	Average	Range	Average	Range
Curvature ↓	3.47	[0.20, 36.79]	2.89	[0.51, 9.17]
Hard Brakes ↓	97.46	[19, 300]	43.62	[19, 89]
Steer Reversals ↓	0.20	[0.01, 0.64]	0.19	[0.06, 0.32]

Table 5: A comparison of traffic rule violations between benign driving and adversarial hijacking under the influence of JACKZEBRA.

Traffic Rule	Benign Driving	Adversarial Hijacking
Red Light ↓	0/7	0/7
Stop Sign ↓	0/5	2/5

vehicle starts, the victim vehicle needs to stop again to follow the traffic rule. This needs fine-grained control of adversarial patches on the adversarial vehicle. In both violations, the victim vehicle only stops once, but not the second time. We argue that while this is a violation of the traffic rule, such a rolling stop [3] happens among human drivers as well.

**Takeaway for RQ3:** JACKZEBRA is stealthy, i.e., the victim’s behavior is similar to that of a normal autonomous driving following the adversarial routes. Exceptions are that the hijacked victim vehicle breaks two stop sign rules by making rolling stops after the adversarial vehicle stops.

## 6 Related Work

**Adversarial attacks on vision-based AV perception:** A large body of work has shown the viability of manipulating camera facing learning components in autonomous driving through physically realizable inputs, even if the attacker does not have access to the model’s internals. Sato et. al. [26] have shown that even benign-appearing manipulations to the road’s surface can cause adversarial bias in deep lane centering pipelines, resulting in sustained lateral control errors and safety violations in the physical world. In addition to lane keeping, attacks also aim at high-impact perception primitives such as traffic signal understanding and depth-based obstacle avoidance. For instance, Rolling Colors [35] indicates that systematic failures in traffic light understanding can be achieved through laser-based attacks that are feasible in optical settings.

Beyond single-camera pipelines, recent work shows that *multisensor fusion* does not eliminate physical-world risk: coordinated physical perturbations can induce consistent errors across camera and LiDAR streams [10], and black-box LiDAR spoofing can be shaped to remain compatible with

camera cues to bypass fusion-level sanity checks [13]. Attacks on traffic sign recognition further demonstrate that robust and physically realizable perturbations can be transferred between viewpoints and environmental variation [15]. In the same manner, Zhou et. al. [39] emphasize the threat of long range manipulation against monocular and stereo depth estimation in obstacle avoidance, noting that distance, perspective, and sensor limitations must be carefully modeled to assess the feasibility of such attacks. GlitchHiker [17] has further expanded the threat model from semantic visual features to the *camera pipeline* and *runtime properties* that perception systems take for granted. On the other hand,  $\pi$ -Jack [38] shows that standard 3D objects can be arranged to subvert the perspective cues used by monocular depth estimation. Recent work [40] also studies how to *improve the physical robustness* of adversarial objects, highlighting that the attack surface includes both generating effective perturbations and ensuring that they remain stable under real-world sensing transformations. Finally, Muller et al. [20] show that attackers can leverage *latency* instead of misclassification by employing projector based perturbations to increase the workload of detectors and introduce latency in perception, forming a viable denial-of-service attack channel against camera-based pipelines. These studies collectively inform the need for assessments that (i) factor in physical limitations (distance, optics, viewpoint), (ii) address pipeline and temporal aspects, and (iii) assess closed-loop safety effectiveness in addition to frame-level accuracy.

**Non-Vision attacks on autonomous vehicles:** Alongside camera-focused threats, non-vision attacks impact autonomous vehicles by exploiting in-vehicle networks, planning logic, and non-camera sensors like LiDAR. For the vehicle network, CANflict [11] illustrates how attackers can leverage peripheral conflicts to carry out data-link layer attacks against vehicle networks. Recent work also advances *practical CAN-bus defenses* that operate within tight performance constraints and legacy framing, e.g., ZBCAN [28], and complements detection with *attack-source identification* on real vehicles, e.g., RIDAS [30]. At the decision-making layer, Wan et al. [33] identify semantic DoS vulnerabilities in autonomous driving planning under physical world attacks, showing that conservative behavioral planners can be forced into mission-degrading behaviors (e.g. persistent stopping) by carefully crafted, seemingly benign environmental con-

ditions. Other research shows that an adversary vehicle can induce unsafe outcomes *purely through interactive motion*, by searching for adversarial driving maneuvers that remain plausible to observers while triggering closed-loop failures in AV stacks [31]. Another work by [9] proposes physical removal attacks against LiDAR-based AV systems by spoofing or blocking point clouds in such a way that obstacles are not modeled as expected, illustrating how adversaries can manipulate geometric sensing channels directly. In particular, Sato et al. [27] evaluate LiDAR spoofing under realistic driving conditions and address feasibility gaps by studying high-speed and long-distance scenarios. Overall, these non-vision attacks motivate a holistic threat model spanning (i) vehicular networks and ECU interactions, (ii) semantic vulnerabilities in planning/control, and (iii) the physical-layer properties of active sensors.

**Adversarial attacks on learning models:** Autonomous driving systems inherit broader adversarial ML threats that apply to learning-based components across domains, including backdoors and privacy leakage. Backdoor attacks are particularly concerning because they can leave models accurate on benign inputs while enabling targeted misbehavior under rare triggers. Graph Backdoor attack [34] shows that graph neural networks can be backdoored by injecting trigger subgraphs, with attacks that are input-tailored and downstream-model-agnostic, raising concerns for any pipeline that relies on graph-structured learning (e.g., relational reasoning, scene graphs, etc.).

Beyond graphs, backdoors have been shown to be hard to detect even when the attacker does not control labels and must remain stealthy under standard evaluation, e.g., *blind backdoors* [7], and can be amplified using explanation-guided poisoning strategies that explicitly optimize for stealth and trigger effectiveness [29]. In NLP settings, trigger mechanisms based on linguistic-style further expand the design space of the backdoor, causing filtering and sanitization [22]. Recent defenses develop more systematic detection principles for backdoors, including methods that target internal representations and activation structure, e.g. BEATRIX [19], and data-centric detection that aims to identify poisoned subsets that generalize across multiple trained models [21]. As LLMs become integrated into safety-critical pipelines, backdoor threats also extend to code-generation and agentic workflows; CodeBreaker [36] demonstrates easy-to-trigger backdoors against code completion models, while recent work proposes deductive/logic-driven approaches to detect and reason about LLM backdoors [24]. Sneaky Spikes [4] extends the backdoor landscape to spiking neural networks by uncovering stealthy backdoor strategies in neuromorphic data, highlighting that emerging efficient architectures also face analogous integrity risks. At the hardware fault level, Rowhammer-Based Trojan Injection [18] demonstrates that flipping a single bit in full precision models can be sufficient to implant an effective backdoor. In addition, privacy attacks quantify what models reveal about their training data. The enhanced Membership In-

ference attack [37] proposes a hypothesis testing-based auditing framework that strengthens membership inference attacks and analyzes why different attacks succeed, underscoring the privacy risk of training data exposure even when models are deployed as black boxes. For autonomous driving, these general threats imply that robustness must include the full ML life cycle: data collection with curation, pretraining and fine-tuning, model distribution with updates, and hardware-backed deployment, since failures can originate well before the vehicle encounters adversarial road conditions.

## 7 Conclusion

This paper examined a new class of physical-world attacks on vision-based autonomous vehicles: *long-horizon route hijacking*. Unlike prior adversarial patch attacks that primarily induce immediate, short-term failures (e.g., collisions or conspicuous traffic-rule violations), route hijacking targets *route integrity*—the guarantee that an AV reaches its intended destination by executing the intended sequence of navigation decisions.

JACKZEBRA treats visual patches as *steering primitives* rather than one-shot perturbations. JACKZEBRA combines (i) an offline optimization procedure that produces a *bank of patches* robust to viewpoint and contextual variation, and (ii) an online interactive adjustment loop that monitors the victim’s realized motion and switches among patches to maintain the desired long-horizon influence under continual replanning.

Our evaluation in closed-loop simulation demonstrates that physically realizable visual perturbations can be composed into targeted long-horizon route-level manipulation. Across diverse routes and environmental conditions, JACKZEBRA redirects victim vehicles toward attacker-designed destinations while exhibiting limited overt anomalies and maintaining largely plausible driving behavior under our measured proxies (e.g., traffic-rule compliance and comfort-related trajectory statistics). These results indicate that route integrity is a distinct and underexplored security property for camera-centric autonomy stacks, and that defending against physical-world adversarial influence requires mechanisms beyond pointwise perception robustness.

More broadly, our findings motivate defenses that explicitly incorporate long-horizon consistency: multi-sensor corroboration (e.g., vision with map priors and inertial/GNSS cues), temporal anomaly detection over route-level intent, and training objectives that penalize persistent externally-induced biases rather than only instantaneous errors. We hope that this work catalyzes further research on principled notions of route integrity, standardized evaluations for long-horizon autonomy failures, and defenses that make embodied AI systems robust not only to immediate safety hazards but also to stealthy mission-level manipulation.

## Ethical Considerations

Our work presents a vulnerability of agents based on SimLingo. While the vehicle hijacking attack is severe and may bring consequences to real passengers, all the experiments are performed in a simulation environment, particularly using the CARLA [2]. Therefore, our experiments did not include physical vehicles, human bystanders, or real-world infrastructure, and therefore did not pose any immediate risk to public safety.

While we conducted the attack in simulation environments, JACKZEBRA could still be deployed in the physical world. We hope our work helps to recognize the vulnerabilities of these autonomous driving agents before a mass deployment, and hope that the research community can help to find corrective actions against these attacks. We then recognize the following stakeholders: 1) autonomous driving agent developers, 2) agent developers, and 3) end-users.

## Open Science

We commit to Open Science and make our code available for public use. An anonymous link to the code is: <https://anonymous.4open.science/r/JackZebra-4A02>.

## References

- [1] How to avoid hard brake. <https://www.amfam.com/resources/articles/on-the-road/avoid-hard-braking>.
- [2] Open-source simulator for autonomous driving research. <https://carla.org/>.
- [3] Putting a stop to rolling stops. <https://www.lytx.com/blog/putting-a-stop-to-rolling-stops>.
- [4] Gorka Abad, Oğuzhan Ersoy, Stjepan Picek, and Aitor Urbieta. Sneaky spikes: Uncovering stealthy backdoor attacks in spiking neural networks with neuromorphic data. In *Network and Distributed System Security Symposium (NDSS) 2024*, 2024.
- [5] Ahmed Abdo, Sakib Md Bin Malek, Xuanpeng Zhao, and Nael Abu-Ghazaleh. Avmon: Securing autonomous vehicles by learning control invariants and residual prediction. In *2024 Symposium on Vehicle Security and Privacy (VehicleSec)*, 2024.
- [6] Aurora Innovation, Inc. Aurora begins commercial driverless trucking in texas, ushering in a new era of freight. Aurora Investor Relations Press Release, May 2025.
- [7] Eugene Bagdasaryan and Vitaly Shmatikov. Blind backdoors in deep learning models, 2021.
- [8] Baidu, Inc. Baidu announces fourth quarter and fiscal year 2024 results. Baidu Investor Relations Press Release, February 2025.
- [9] Yulong Cao, S. Hrushikesh Bhupathiraju, Pirouz Naghavi, Takeshi Sugawara, Z. Morley Mao, and Sara Rampazzi. You can't see me: Physical removal attacks on LiDAR-based autonomous vehicles driving frameworks. In *32nd USENIX Security Symposium (USENIX Security 23)*, pages 2993–3010, 2023.
- [10] Yulong Cao, Ningfei Wang, Chaowei Xiao, Dawei Yang, Jin Fang, Ruigang Yang, Qi Alfred Chen, Mingyan Liu, and Bo Li. Invisible for both camera and lidar: Security of multi-sensor fusion based perception in autonomous driving under physical-world attacks. In *2021 IEEE Symposium on Security and Privacy (SP)*, pages 176–194, 2021.
- [11] Alvise de Faveri Tron, Stefano Longari, Michele Carmignani, Mario Polino, and Stefano Zanero. Canflict: Exploiting peripheral conflicts for data-link layer attacks on automotive networks. In *Proceedings of the 2022 ACM SIGSAC Conference on Computer and Communications Security (CCS '22)*, 2022.
- [12] Kevin Eykholt, Ivan Evtimov, Earlene Fernandes, Bo Li, Amir Rahmati, Chaowei Xiao, Atul Prakash, Tadayoshi Kohno, and Dawn Song. Robust physical-world attacks on deep learning visual classification. In *2018 IEEE/CVF Conference on Computer Vision and Pattern Recognition*, pages 1625–1634, 2018.
- [13] R. Spencer Hallyburton, Yupei Liu, Yulong Cao, Z. Morley Mao, and Miroslav Pajic. Security analysis of Camera-LiDAR fusion against Black-Box attacks on autonomous vehicles. In *31st USENIX Security Symposium (USENIX Security 22)*, pages 1903–1920, 2022.
- [14] Wei Jia, Zhaojun Lu, Haichun Zhang, Zhenglin Liu, Jie Wang, and Gang Qu. Fooling the eyes of autonomous vehicles: Robust physical adversarial examples against traffic sign recognition systems. *NDSS*, 2022.
- [15] Wei Jia, Zhaojun Lu, Haichun Zhang, Zhenglin Liu, Jie Wang, and Gang Qu. Fooling the eyes of autonomous vehicles: Robust physical adversarial examples against traffic sign recognition systems, 2022.
- [16] Xiaosong Jia, Zhenjie Yang, Qifeng Li, Zhiyuan Zhang, and Junchi Yan. Bench2drive: Towards multi-ability benchmarking of closed-loop end-to-end autonomous driving. In *Advances in Neural Information Processing Systems (NeurIPS 2024), Datasets and Benchmarks Track*, 2024.

[17] Qinhong Jiang, Xiaoyu Ji, Chen Yan, Zhixin Xie, Haina Lou, and Wenyuan Xu. Glitchhiker: Uncovering vulnerabilities of image signal transmission with iemi. In *32nd USENIX Security Symposium (USENIX Security 23)*, 2023.

[18] Xiang Li, Ying Meng, Junming Chen, Lannan Luo, and Qiang Zeng. Rowhammer-based trojan injection: One bit flip is sufficient for backdooring dnns. In *34th USENIX Security Symposium (USENIX Security 25)*, 2025.

[19] Wanlun Ma, Derui Wang, Ruoxi Sun, Minhui Xue, Sheng Wen, and Yang Xiang. The "beatrix" resurrections: Robust backdoor detection via gram matrices, 2022.

[20] Raymond Muller, Ruoyu Song, Chenyi Wang, Yuxia Zhan, Jean-Philippe Monteuius, Yanmao Man, Ming Li, Ryan Gerdes, Jonathan Petit, and Z. Berkay Celik. Investigating physical latency attacks against camera-based perception. In *2025 IEEE Symposium on Security and Privacy (SP)*, 2025.

[21] Minzhou Pan, Yi Zeng, Lingjuan Lyu, Xue Lin, and Ruoxi Jia. Asset: Robust backdoor data detection across a multiplicity of deep learning paradigms, 2023.

[22] Xudong Pan, Mi Zhang, Beina Sheng, Jiaming Zhu, and Min Yang. Hidden trigger backdoor attack on NLP models via linguistic style manipulation. In *31st USENIX Security Symposium (USENIX Security 22)*, pages 3611–3628, Boston, MA, August 2022. USENIX Association.

[23] Kexin Pei, Yinzhi Cao, Junfeng Yang, and Suman Jana. Deepxplore: automated whitebox testing of deep learning systems. *Commun. ACM*, 62(11):137–145, October 2019.

[24] Dorde Popovic, Amin Sadeghi, Ting Yu, Sanjay Chawla, and Issa Khalil. Debackdoor: A deductive framework for detecting backdoor attacks on deep models with limited data, 2025.

[25] Katrin Renz, Long Chen, Elahe Arani, and Oleg Sinavski. Simlingo: Vision-only closed-loop autonomous driving with language-action alignment. In *Proceedings of the Computer Vision and Pattern Recognition Conference*, pages 11993–12003, 2025.

[26] Takami Sato, Junjie Shen, Ningfei Wang, Yunhan Jia, Xue Lin, and Qi Alfred Chen. Dirty road can attack: Security of deep learning based automated lane centering under Physical-World attack. In *30th USENIX Security Symposium (USENIX Security 21)*, pages 3309–3326. USENIX Association, August 2021.

[27] Takami Sato, Ryo Suzuki, Yuki Hayakawa, Kazuma Ikeda, Ozora Sako, Rokuto Nagata, Ryo Yoshida, Qi Alfred Chen, and Kentaro Yoshioka. On the realism of lidar spoofing attacks against autonomous driving vehicle at high speed and long distance. In *Network and Distributed System Security Symposium (NDSS) 2025*, 2025.

[28] Khaled Serag, Rohit Bhatia, Akram Faqih, Muslum Ozgur Ozmen, Vireshwar Kumar, Z. Berkay Celik, and Dongyan Xu. ZBCAN: A Zero-Byte CAN defense system. In *32nd USENIX Security Symposium (USENIX Security 23)*, pages 6893–6910, Anaheim, CA, August 2023. USENIX Association.

[29] Giorgio Severi, Jim Meyer, Scott Coull, and Alina Oprea. Explanation-Guided backdoor poisoning attacks against malware classifiers. In *30th USENIX Security Symposium (USENIX Security 21)*, pages 1487–1504. USENIX Association, August 2021.

[30] Jiwoo Shin, Hyunghoon Kim, Seyoung Lee, Wonsuk Choi, Dong Hoon Lee, and Hyo Jin Jo. RIDAS: Real-time identification of attack sources on controller area networks. In *32nd USENIX Security Symposium (USENIX Security 23)*, pages 6911–6928, Anaheim, CA, August 2023. USENIX Association.

[31] Ruoyu Song, Muslum Ozgur Ozmen, Hyungsuk Kim, Raymond Muller, Z. Berkay Celik, and Antonio Bianchi. Discovering adversarial driving maneuvers against autonomous vehicles. In *32nd USENIX Security Symposium (USENIX Security 23)*, pages 2957–2974, Anaheim, CA, August 2023. USENIX Association.

[32] The Waymo Team. Safe, routine, ready: Autonomous driving in five new cities. *Waymo Blog*, November 2025.

[33] Ziwen Wan, Junjie Shen, Jalen Chuang, Xin Xia, Joshua Garcia, Jiaqi Ma, and Qi Alfred Chen. Too afraid to drive: Systematic discovery of semantic dos vulnerability in autonomous driving planning under physical-world attacks. In *Network and Distributed System Security Symposium (NDSS) 2022*, 2022.

[34] Zhaohan Xi, Ren Pang, Shouling Ji, and Ting Wang. Graph backdoor. In *30th USENIX Security Symposium (USENIX Security 21)*, pages 1523–1540, 2021.

[35] Chen Yan, Zhijian Xu, Zhanyuan Yin, Xiaoyu Ji, and Wenyuan Xu. Rolling colors: Adversarial laser exploits against traffic light recognition. In *31st USENIX Security Symposium (USENIX Security 22)*, pages 1957–1974, 2022.

- [36] Shenao Yan, Shen Wang, Yue Duan, Hanbin Hong, Kiho Lee, Doowon Kim, and Yuan Hong. An LLM-Assisted Easy-to-Trigger backdoor attack on code completion models: Injecting disguised vulnerabilities against strong detection. In *33rd USENIX Security Symposium (USENIX Security 24)*, pages 1795–1812, Philadelphia, PA, August 2024. USENIX Association.
- [37] Jiayuan Ye, Aadyaa Maddi, Sasi Kumar Murakonda, Vincent Bindschaedler, and Reza Shokri. Enhanced membership inference attacks against machine learning models. In *Proceedings of the 2022 ACM SIGSAC Conference on Computer and Communications Security (CCS '22)*, 2022.
- [38] Tianyue Zheng, Jingzhi Hu, Rui Tan, Yinqian Zhang, Ying He, and Jun Luo.  $\pi$ -jack: Physical-world adversarial attack on monocular depth estimation with perspective hijacking. In *33rd USENIX Security Symposium (USENIX Security 24)*, 2024.
- [39] Ce Zhou, Qiben Yan, Yan Shi, and Lichao Sun. DoubleStar: Long-Range attack towards depth estimation based obstacle avoidance in autonomous systems. In *31st USENIX Security Symposium (USENIX Security 22)*, pages 1885–1902, 2022.
- [40] Shencheng Zhu, Yue Zhao, Kai Chen, Bo Wang, Hualong Ma, and Cheng'an Wei. AE-Morpher: Improve physical robustness of adversarial objects against LiDAR-based detectors via object reconstruction. In *33rd USENIX Security Symposium (USENIX Security 24)*, pages 7339–7356, Philadelphia, PA, August 2024. USENIX Association.